



Early immunopathological events in acute model of mycobacterial hypersensitivity pneumonitis in mice

Elisabet Johansson, Gregory P. Boivin & Jagjit S. Yadav

To cite this article: Elisabet Johansson, Gregory P. Boivin & Jagjit S. Yadav (2017) Early immunopathological events in acute model of mycobacterial hypersensitivity pneumonitis in mice, *Journal of Immunotoxicology*, 14:1, 77-88, DOI: [10.1080/1547691X.2016.1273284](https://doi.org/10.1080/1547691X.2016.1273284)

To link to this article: <https://doi.org/10.1080/1547691X.2016.1273284>



© 2017 The Author(s). Published by Informa UK Limited, trading as Taylor & Francis Group



Published online: 17 Jan 2017.



Submit your article to this journal 



Article views: 447



View Crossmark data 

Early immunopathological events in acute model of mycobacterial hypersensitivity pneumonitis in mice

Elisabet Johansson^a, Gregory P. Boivin^b and Jagjit S. Yadav^a

^aDepartment of Environmental Health, Microbial Pathogenesis and Immunotoxicology Laboratory, Division of Environmental Genetics and Molecular Toxicology, University of Cincinnati College of Medicine, Cincinnati, OH, USA; ^bDepartment of Pathology and Orthopedic Surgery, Wright State University, Dayton, OH, USA

ABSTRACT

Prolonged exposure to antigens of non-tuberculous mycobacteria species colonizing industrial metalworking fluid (MWF), particularly *Mycobacterium immunogenum* (MI), has been implicated in chronic forms of hypersensitivity pneumonitis (HP) in machinists based on epidemiology studies and long-term exposure of mouse models. However, a role of short-term acute exposure to these antigens has not been described in the context of acute forms of HP. This study investigated short-term acute exposure of mice to MI cell lysate (or live cell suspension) via oropharyngeal aspiration. The results showed there was a dose- and time-dependent increase (peaking at 2 h post-instillation) in lung immunological responses in terms of the pro-(TNF α , IL-6, IL-1 β) and anti-inflammatory (IL-10) cytokines. Bronchoalveolar lavage and histology showed neutrophils as the predominant infiltrating cell type, with lymphocytes <5% at all timepoints or concentrations. Granulomatous inflammation peaked between 8 and 24 h post-exposure, and resolved by 96 h. Live bacterial challenge, typically encountered in real-world exposures, showed no significant differences from bacterial lysate except for induction of appreciable levels of interferon (IFN)- γ , implying additional immunogenic potential. Collectively, the short-term mycobacterial challenge in mice led to a transient early immunopathologic response, with little adaptive immunity, which is consistent with events associated with human acute forms of HP. Screening of MWF-originated mycobacterial genotypes/variants (six of MI, four of *M. chelonae*, two of *M. abscessus*) showed both inter- and intra-species differences, with MI genotype MJY10 being the most immunogenic. In conclusion, this study characterized the first short-term mycobacterial exposure mouse model that mimics acute HP in machinists; this could serve as a potentially useful model for rapid screening of field MWF-associated mycobacteria for routine and timely occupational risk assessment and for investigating early biomarkers and mechanisms of this understudied immune lung disease.

ARTICLE HISTORY

Received 21 October 2016
Revised 12 December 2016
Accepted 13 December 2016

KEYWORDS

Mycobacterium immunogenum; hypersensitivity pneumonitis; metalworking fluid; inhalation; acute exposure; mouse; bronchoalveolar lavage; cytokines; lung pathology; immunopathological changes

Introduction

Hypersensitivity pneumonitis (HP) is an immunologic lung disease that can present in any of the three clinical forms *viz.* acute, subacute, or chronic (Costabel et al. 2012; Selman & Buendia-Roldan 2012). HP is caused by the inhalation of a wide variety of antigenic particles small enough to reach the alveoli, comprised of microbial, animal, or insect proteins and other constituents. Environmental mycobacteria of the *M. chelonae*–*M. abscessus* (MCA) group – particularly *M. immunogenum* – have been associated with outbreaks of HP in factory workers inhalationally exposed to contaminated metalworking fluid (MWF) aerosols (Kreiss & Cox-Ganser 1997; Moore et al. 2000; Wilson et al. 2001; Falkinham 2003; Beckett et al. 2005; Tillie-Leblond et al. 2011). HP cases presenting variable clinical forms (acute, subacute, chronic) have been observed in machinists exposed to contaminated MWF (Freeman et al. 1998; Zacharisen et al. 1998; Beckett et al. 2005; Rosenman 2009). While there has been increasing interest in both clinical and research aspects of MWF-associated HP (Gupta et al. 2009; Tillie-Leblond et al. 2011; Roussel et al. 2011; Burton et al. 2012; Chandra et al. 2013, 2015), differential

diagnosis and immunological mechanisms of this occupational lung disease are still poorly understood.

HP is a complex Type III/Type IV hypersensitivity disease where immune response to initial inhalation of provoking antigens is believed to be immune complex-mediated (Type III response), while prolonged and repeated exposure results in a cell-mediated Type IV hypersensitivity response (Mohr 2004). Subacute and chronic HP forms in humans are characterized by granuloma formation, lymphocytic infiltration, and in the case of chronic HP form, interstitial and peribronchial fibrosis is prominent. The histopathological features of acute HP, on the other hand, are less well described (Grunes & Beasley 2013). This may be in large part due to the rapid onset of acute HP after exposure to large doses of provoking antigens followed by rapid resolution of symptoms once exposure ceases, and as a consequence of the rapid recovery, biopsies are rarely performed (Selman et al. 2012). This raises the need to develop appropriate experimental models of acute HP.

Animal models of HP are mainly based on the use of antigens derived from the actinomycete *Saccharopolyspora rectivirgula*, which in humans is the cause of Farmer's lung, a common form

CONTACT Dr. Jagjit S. Yadav  jagjit.yadav@uc.edu  Department of Environmental Health, University of Cincinnati College of Medicine, Kettering Laboratory Complex, 160 Panzica Way, Cincinnati, OH 45267-0056, USA

© 2017 The Author(s). Published by Informa UK Limited, trading as Taylor & Francis Group

This is an Open Access article distributed under the terms of the Creative Commons Attribution License (<http://creativecommons.org/licenses/by/4.0/>), which permits unrestricted use, distribution, and reproduction in any medium, provided the original work is properly cited.

of HP affecting farmers. The most common subchronic/chronic murine model of HP involves the nasal instillation of mice with *S. rectivirgula* antigen on three consecutive days per week for three weeks, which results in a strong T-helper cell Type 1 (T_{H1})-driven immune response and granuloma formation (Denis et al. 1991; Gudmundsson & Hunninghake 1998; Nance et al. 2004; Jimenez-Alvarez et al. 2010). More recently, *M. immunogenum* isolated from contaminated MWFs has also been shown to induce chronic HP-like pathology in mice instilled according to the same regimen (Gordon et al. 2006; Thorne et al. 2006). However, there are no studies yet on acute HP mouse model for MWF mycobacteria-linked machinist HP. A few acute or short-term exposure protocols using *S. rectivirgula* as the antigen have demonstrated strong neutrophilic infiltration, and identified neutrophils as a source of interferon (IFN)- γ sufficient for granuloma formation (Schuyler et al. 1994; Nance et al. 2005). Other reports also indicated the presence of limited delayed lymphocytosis in acute HP (Schuyler 1993; Hunninghake & Richerson 1998; Schuyler et al. 2000).

Thus, development of a more specific animal model that closely mimics human acute HP characteristics in machinists could further help elucidate the early events and detailed immune-pathological features of acute HP. For instance, the immune responses and lung pathologies detected in animal models of HP depend to a great extent on time of sacrifice after last instillation (Jimenez-Alvarez et al. 2010), and early immunopathologic responses may be undetected when sacrifice is performed at the 4-day timepoint commonly used (Gordon et al. 2006; Thorne et al. 2006). Furthermore, existing mouse challenge studies on MWF-associated HP have been restricted to the use of one particular causative bacterial species and have not reported species/strain-dependent variation in immunogenicity and severity of the disease (Gordon et al. 2006; Thorne et al. 2006). Large-scale screening of field-collected MWF samples by our laboratory has revealed prevalence of different species (*M. immunogenum*, *M. chelonae*, *M. abscessus*) of the MCA group and several unique genotypes/variants of each of these member species (Khan et al. 2005; Kapoor & Yadav 2012) in these fluids. However, the relative immunogenicity and HP-inducing potential of individual mycobacterial genotypes/variants is unclear.

The objective of the study reported here was to characterize the response to short-term exposure of the T_{H1} -biased mouse inbred strain C57BL/6J to *M. immunogenum* as a function of instillation dose and post-exposure time of sacrifice with intent to optimize a short-term exposure mouse model of mycobacterial HP that mimics acute HP characteristics. An additional goal was to compare intact live bacterial cells with whole cell lysates to understand the role of cellular context of the causative agent (*M. immunogenum*) as prevalent in a real-world exposure scenario. A further goal was to compare the unique collection of 12 distinct strains (genotypes/variants) of MWF-associated mycobacteria species *M. immunogenum*, *M. chelonae*, and *M. abscessus* previously isolated from field industrial MWF in our laboratory, to understand their relative immunogenicity and HP-inducing potential in the developed experimental HP model.

Materials and methods

Mice

C57BL/6J mice (male, 6–8-wk-old) were purchased from the Jackson Laboratory (Bar Harbor, ME). Mice were housed in PIV cages under pathogen-free conditions maintained at 22–24 °C with a 40–43% relative humidity and a 12 h light:dark cycle.

All mice had *ad libitum* access to standard rodent chow and filtered water. All experimental protocols used here were approved by the Institutional Animal Care and Use Committee of the University of Cincinnati.

Bacterial strains and culture conditions

Three member species of the *M. chelonae*–*M. abscessus* group of non-tuberculous mycobacteria, i.e. *M. immunogenum*, *M. chelonae*, *M. abscessus* originally isolated from field in-use or used MWFs from geographically diverse automotive industrial plants (Khan et al. 2005; Kapoor & Yadav 2012) were used in these studies. A total of 12 strains/genotypes belonging to these three species, including six *M. immunogenum* genotypes (MI 700506, MJY3, MJY4, MJY10, MJY13, and MJY14), four *M. chelonae* genotypes (MJY1, MJY2, MJY6, and MJY8), and two *M. abscessus* strains/morphotypes, rough (MJY23) and smooth (MJY25), were included. The mycobacterial species and genotypes/variants were grown in Middlebrook 7H9 medium (BD Diagnostics, Sparks, MD) supplemented with 10% *Oleic Albumin Dextrose Catalase* (OADC) enrichment (BD Diagnostics, Sparks, MD) unless otherwise indicated. The actinomycete *Saccharopolyspora rectivirgula* used for comparison studies was grown to generate a whole cell lysate, as described previously (Gudmundsson & Hunninghake 1998).

Preparation of challenge inoculum

Mycobacterial cell extracts

Using continuous shaking at 200 rpm, *M. immunogenum* 700506 was grown at 37 °C and all other mycobacterial strains were grown at 30 °C in Middlebrook 7H9 broth supplemented with 10% OADC enrichment (BD Biosciences, Sparks, MD). When a reading of 120 Klett units was reached, as measured in a Klett–Summerson photoelectric colorimeter (Klett Manufacturing Co., New York, NY), cells were pelleted by centrifugation at 3000 \times g, and washed three times with certified endotoxin-free phosphate-buffered saline (PBS, pH 7.4). The resulting cell pellet was resuspended in endotoxin-free PBS, and one ml cell suspension was added to a sterile 2-ml tube containing 0.4 g acid-washed glass beads. The tube was shaken in a Mini-Bead beater (Biospec Products, Bartlesville, OK) four times (each for 1 min) with cooling on ice for 2 min in between. The resulting homogenate was decanted from the beads, and the protein concentration then determined using a DCTM protein assay from BioRad (Hercules, CA). Resulting whole cell extracts were frozen at –80 °C until further use.

Monodispersed mycobacterial cells

For the preparation of a monodispersed cell suspension, *M. immunogenum* 700506 was grown to a density of 120 Klett units as described above, except that the growth medium was Sauton's broth containing 0.1% Tween-80 prepared in-house per the following composition: L-asparagine (4 g/L), citric acid (2 g/L), K₂HPO₄ (0.5 g/L), MgSO₄ (0.5 g/L), ferric ammonium citrate (0.05 g/L), glycerol (35 ml/L), and Tween-80 (1 ml/L); pH was adjusted to 7.2 using NaOH solution. The cells were washed three times with endotoxin-free PBS, and resuspended in the same medium. The cell suspension was repeatedly passed through a 23-G needle (10 times), and then through a 26-G needle (10 times). The resulting cell suspension was centrifuged

5 min at $100 \times g$, and the supernatant aspirated off. Bacterial count (in terms of colony-forming units [cfu]/ml) of this mono-dispersed suspension was determined by plating aliquots of various dilutions on Middlebrook 7H10 agar supplemented with 10% OADC enrichment (BD Biosciences).

Oropharyngeal instillation regimen

Oropharyngeal aspiration method was used to expose the mice ($n=8$ /group for the optimization experiments; $n=5$ /group for viable cell exposure; $n=4-5$ /group for genotype screen) to bacterial cells or extracts. The mice were anesthetized using isoflurane, and suspended on a restraining board tilted backwards 45° . The tongue was gently pulled out with tweezers, 50 μ l antigen were added to the base of the tongue, and the nares were immediately blocked to force inhalation through the mouth. Instillations were done on three consecutive days, once per day for a total of three instillations. With the exception of the time-course study, the mice were then euthanized at 4 h after the final instillation by intraperitoneal injection of EuthasolTM. At necropsy, the lungs were lavaged with 2×1 -ml Ca^{2+} , Mg^{2+} -free PBS; the two aliquots were then combined. The lavaged lungs were then placed in formalin for 24 h. The lavage fluid was centrifuged at 4°C for 10 min at $300 \times g$ and the resulting supernatant then recovered and stored at -80°C until further use. The cell pellet was re-suspended in PBS containing 5% fetal bovine serum (Atlanta Biologicals, Flowery Branch, GA) and the cells then counted in hemocytometer to obtain total numbers in bronchoalveolar lavage fluid (BALF). Differential cell counts were obtained by counting >300 cells on cytocentrifuge preparations (Cytospin3; Shandon Scientific, Cheshire, UK) after staining using a Hema 3 kit (Fisher Scientific, Waltham, MA).

BALF analyses

Protein concentrations in BALF samples were determined using a DCTM protein assay (BioRad). The BALF were also analyzed for various cytokines, e.g. IFN γ , tumor necrosis factor (TNF)- α , interleukin (IL)-1 β , IL-6, IL-10, and IL-12 using Ready-Set-Go![®] ELISA kits (eBioscience, San Diego, CA), according to the manufacturer instructions. The level of sensitivity of the kits was 15 pg IFN γ /ml, 8 pg TNF α /ml, 8 pg IL-1 β /ml, 4 pg IL-6/ml, 15 pg IL-10/ml, and 15 pg IL-12/ml. All samples were analyzed in triplicate.

Histopathology

The formalin-fixed lungs were processed to yield 5- μm sections that were then stained using H&E. Analysis on three random slides/group was then performed in a blinded manner using a light microscope. Various pathological features including peribronchial/perivasculair infiltration, alveolar infiltration, granuloma formation, and overall severity were scored on a subjective scale of 0-4 as: 0 = no inflammation; 0.5 = very mild; 1 = mild; 2 = moderate; 3 = severe; 4 = very severe. Overall extensiveness of the lung involvement was scored on the same scale as follows: 0 = no inflammation; 1 = 0-10%; 2 = 10-30%; 3 = 30-50%; 4 = $>50\%$.

Statistical analyses

Statistical analysis was performed using SigmaStat software (SPSS Inc, Chicago, IL). Log transformation of variables was performed

when necessary to obtain normal distribution. Group means were compared by one-way analysis of variance (ANOVA). Multiple comparisons vs. control group, according to Dunn's Method, were used for *post-hoc* testing of significance in the time-course and dose-response analyses. A Holm-Sidak *post-hoc* test of significance – including all pairwise comparisons – was used in analyses of the 12 different genotypes. A Kruskal-Wallis analysis of variance on ranks was used to analyze the histopathological scores. Data are reported as means \pm SE. For all analyses, the α level for statistical significance was $p < 0.05$.

Results

Time-course of lung responses to MI cell extract

Inflammatory and histopathological metrics were studied as functions of the timepoint of sacrifice after the last instillation of MI dose. The timepoints ranged from 2 to 96 h, and the dose of mycobacterial protein was 6 μg per instillation. The protein concentration in BALF was increased 3.5-fold at 2 h, and remained at this level for 24 h, returning to base level at 96 h (Figure 1(A)). The total number of cells in BALF followed a similar pattern, although the increase at 2 h was not statistically significant as compared with the base level, nor was the net remaining increase at 96 h (Figure 1(B)). The total number of neutrophils peaked between 4 and 12 h, whereas the levels of macrophages and lymphocytes were highest at the 24-h timepoint (Figure 1(C)). The cytokines TNF α , IL-6, IL-10, and IL-1 β in BALF showed a sharp increase at 2 h, followed by decrease back to background levels albeit at a variable pace. Levels of TNF α and IL-6 showed a steady decrease back to background levels near the 24 h timepoint (Figure 1(D,E)). IL-1 β levels showed a sharp decrease after 2 h but remained steady until 12 h, returning to background by 24 h (Figure 1(G)). However, IL-10 levels remained elevated through 24 h and returned to near background levels at 96 h (Figure 1(F)). IFN γ levels were not above the background level at any timepoint (data not shown).

Histopathology analysis showed a very mild-to-mild granuloma formation that peaked at 8-12 h after the final instillation, decreasing slowly after that (Figure 2(A)) and resolving by 96 h. Peribronchial and perivasculair infiltration which was primarily neutrophilic, was moderate at the 2 h point, and regressed to very mild-to-mild at the subsequent timepoints. Only some mice had alveolar infiltration ($\approx 50\%$ at 4-24 h timepoints). Overall severity of the histopathologic lesions showed a significant gradual decrease from 2 h to 96 h post-instillation, whereas the overall extensiveness of lesions in the lung remained constant (Figure 2(B)).

Dose-response relationship (using MI whole cell extract)

The inflammatory response to varying MI (cell extract) doses (0.2-60 μg) of mycobacterial protein was measured at 4 h post-final instillation. Total protein content in collected BALF showed a gradual increase between 0.6 and 20 μg MI protein dose range, but a strong increase (to 2.4 mg/ml) at 60 μg MI protein dose (Figure 3(A)). Total numbers of cells in BALF also showed a gradual increase beginning with the 0.6 μg MI dose and a subsequent sharp increase (to 2.9×10^6 cells) at 20 μg (Figure 3(B)). The cell count decreased, however, to 1.4×10^6 at the highest dose (60 μg). Though macrophages and lymphocytes showed mild increases, the majority of the increase in total cell count was due to an influx of neutrophils (Figure 3(C)). TNF α and

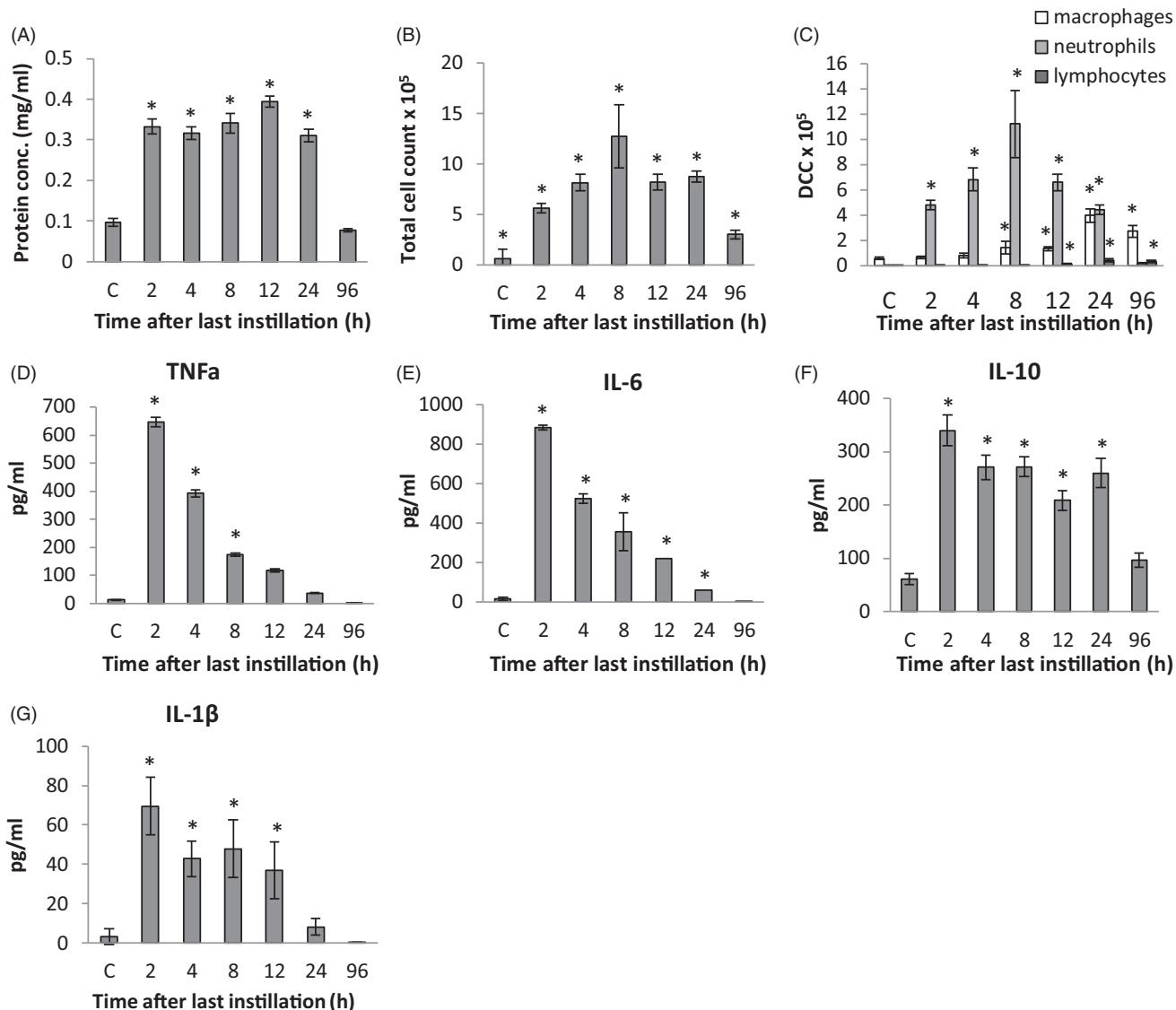


Figure 1. Effect of post-instillation time on immunological changes in mouse lung after oropharyngeal exposure to whole cell lysate of *M. immunogenum* 700506. Dose (in terms of mycobacterial protein) was 6 μ g/instillation. BALF was collected at different timepoints (as shown in hours on the X-axis) post-instillation of final dose. Panels A-C: Biochemical and cellular changes in BALF: (A) Total protein concentration; (B) Total immune cell counts; and, (C) Differential cell counts (DCC) of immune cells. Panels D-G: BALF levels of (D) TNF α , (E) IL-6, (F) IL-10, and (G) IL-1 β . *Value significantly different from control ($p \leq 0.05$).

IL-6 showed an increase beginning at 0.6 μ g (Figure 3(D,E)) that gradually increased and showed a dramatic increase beginning at 20 μ g. The levels of IL-10 showed a steady increase over the entire 0.6–60 μ g dose range (Figure 3(F)). IL-1 β levels were mildly increased beginning at 6 μ g and showed a steady increase thereafter (Figure 1(G)). In contrast to other cytokines, IFN γ levels were not significantly increased above background at any dose (data not shown).

The inflammation was primarily restricted to the perivascular and peribronchiolar regions with granulomas in the alveoli and diffuse inflammation in alveolar lumens (Figure 4). Granuloma formation was observed beginning with the 2 μ g mycobacterial protein dose, with moderate granuloma formation at 20 μ g, and severe granuloma formation at 60 μ g (Figure 4(A,D,E)). Peribronchial and perivascular infiltration was seen at doses of 0.2 μ g and above, and was primarily neutrophilic. There was diffuse neutrophilic infiltration into the alveoli separate from the granulomas starting at 2 μ g. Both the overall severity and the

extensiveness of lung lesions showed a significant increase over the 0.2–60 μ g test dose range (Figure 4(B)).

Dose-response relationship (using MI live cell suspension)

Responses to intact live cells of *M. immunogenum* were investigated using three doses (i.e. 10^6 , 10^7 , and 2.5×10^7 cells; expressed as cfu) that corresponded to 0.24, 2.4, and 6 μ g, respectively, of whole cell extract protein preparation used in the preceding experiments. BALF protein levels were significantly increased at the two highest MI doses, but not at the lowest (10^6 cfu) dose (Figure 5(A)). The cellularity of the BALF in terms of total cell count of the immune cells followed the same pattern (Figure 5(B)). Differential cell counts from the BALF however showed a steady increase in macrophages at all test doses, with the highest dose causing significant increase (Figure 5(C)), and a strong significant increase in neutrophils at the two highest doses (from basal count of 0.5×10^3 cells in controls to 1.9×10^5 and 4.8×10^5 cells at the 10^7 and

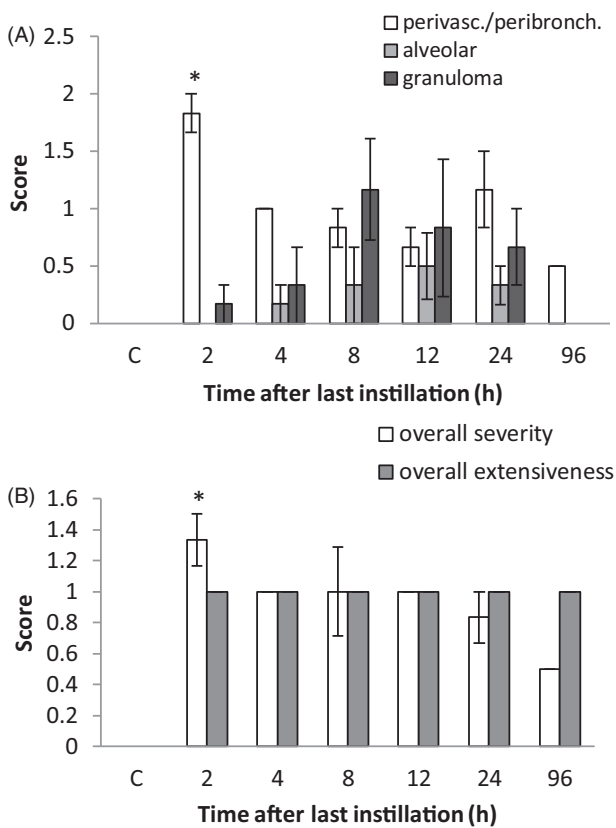


Figure 2. Effect of post-instillation time on histopathological changes in mouse lung after oropharyngeal exposure to whole cell lysate of *M. immunogenum* 700506. Specific histopathological changes measured were: Panel A: Peribronchial and perivascular infiltration, alveolar infiltration, and granuloma formation. Panel B: Overall severity/overall extensiveness of histopathological lesions. Dose (as mycobacterial protein) was 6 µg/instillation. Analysis was performed on tissues harvested at different timepoints (as shown in hours on X-axis) post-instillation of final dose. Changes in the lung were evaluated in terms of overall scores for severity and extensiveness of pathology, as well as scores for specific histopathological changes, assigned on a subjective scale of 0–4 as described under Materials and methods section. *Significantly different from control ($p \leq 0.05$).

2.5×10^7 cfu doses, respectively). Although there was a significant increase in numbers of lymphocytes at the highest dose, lymphocytes did not account for >4% of the total number of cells in the BALF. Levels of TNF α and IL-6 in BALF both were significantly increased with dose, particularly at the two highest doses (Figure 5(D,E)). BALF IL-1 β levels were mildly but significantly increased at the two highest doses (Figure 5(F)). BALF levels of IFN γ were very slightly increased with dose, with a significant increase at the highest dose (Figure 5(G)). Anti-inflammatory IL-10 in BALF was not increased with any dose (data not shown).

Perivascular and peribronchial infiltration ranged from very mild-to-mild and was mixed neutrophilic/lymphocytic at the 10^7 cfu dose, and primarily lymphocytic at 2.5×10^7 cfu (Figure 6(A)). Alveolar infiltration was primarily neutrophilic or mixed and very mild at 10^7 cfu and mild-to-moderate with the 2.5×10^7 cfu dose. No significant granuloma formation was seen with any of the test doses. The overall severity and extensiveness of lung lesions ranged from very mild-to-moderate for the two highest doses (Figure 6(B)).

Comparative immunopathological responses to mycobacterial genotypes/variants

The relative responses in C57BL/6J mice to different mycobacterial genotypes/variants were investigated for six *M. immunogenum*

genotypes (MI 700506, MJY3, MJY4, MJY10, MJY13, and MJY14), four *M. chelonae* genotypes (MJY1, MJY2, MJY6, and MJY8), and two *M. abscessus* morphotypes (MJY23 and MJY25). Animals instilled with *S. rectivirgula* and endotoxin-free PBS served as positive and negative (vehicle) controls, respectively.

Immunological responses

Total protein content in the BAL fluids from treated animals was significantly elevated relative to the vehicle control animals in all treatment groups except the MJY14 group (Figure 7(A)). Animals instilled with MJY10 had protein levels that were significantly higher than all other groups except MJY8 and MI 700506 (overall ANOVA $p < 0.001$), while the group with the lowest protein levels, MJY14, had values that were significantly lower than groups MI 700506, MJY1, MJY8, MJY10, MJY25, and the comparison control *S. rectivirgula* ($p < 0.001$). In terms of cellularity, the total cell count in BAL fluid was increased in all groups, though increases were only statistically significant for groups MJY1, MJY3, MJY8, and MJY10 (Figure 7(B)). The group with the highest cell number, MJY10, had counts that were significantly higher than those for groups MI 700506, MJY2, MJY6, MJY23, MJY25, and *S. rectivirgula*.

Differential cell counts of immune cells in BALF showed that all treated mice (except vehicle controls) had pronounced neutrophilic infiltration in airspaces, with neutrophils accounting for 80–95% of total cell numbers (Figure 7(C)). The MJY10 group had the highest number of neutrophils/ml BALF (17.6×10^5), a level significantly higher than the total neutrophils in the BALF from the MJY2, MJY6, MJY14, MJY23, MJY25, MI 700506, and *S. rectivirgula* groups. The number of macrophages in BALF was mildly elevated in only a few groups, with the MJY1 and MJY10 groups having significantly higher counts than the MJY4, MJY6, and *S. rectivirgula* groups. While lymphocyte numbers in BALF were slightly elevated in all groups, the increase was only significant for the MJY6 ($p = 0.026$), MJY8 ($p = 0.007$), and MJY10 ($p = 0.002$) groups; in none of the groups did lymphocytes account for >5% of total number of cells in BALF.

BALF cytokine levels showed variable changes (Figure 8). IFN γ levels were significantly though mildly increased in the MJY10, MI 700506, and *S. rectivirgula* groups (to 45.3, 27.2, and 76.6 pg/ml, respectively) from control levels of 9.3 pg/ml (Figure 8(A)). Levels of TNF α were increased in all groups relative to the vehicle control (3.2 pg/ml) (Figure 8(B)). The MJY10 group had a mean TNF α concentration of 1241 pg/ml, significantly higher than that for all other treatment groups except MJY2 and MJY6 ($p < 0.05$). The MJY14 group had the lowest mean TNF α concentration (203 pg/ml), which was significantly lower than that for all other treatment groups except MJY1, MJY8, MJY23, and MJY25. BALF IL-12 levels were mildly but significantly increased in all groups relative to vehicle control (4.7 pg/ml) (Figure 8(C)). *S. rectivirgula*, the comparison control group (positive control), had the highest level (468 pg/ml) and was significantly ($p < 0.05$) greater than values in all other groups except MJY6, MJY10, and MI 700506. Among the mycobacterial strains, MJY10 resulted in the highest IL-12 concentration, (210 pg/ml), a value significantly higher than that seen in the MJY1 and MJY14 groups. IL-10 levels were highly variable; though concentrations trended higher in all groups relative to the vehicle control (4.6 pg/ml), the increase was only statistically significant for groups MJY1, MJY10, and MI 700506, and the comparison control (*S. rectivirgula*) group (337 pg/ml). Among the mycobacterial genotypes/variants, MI

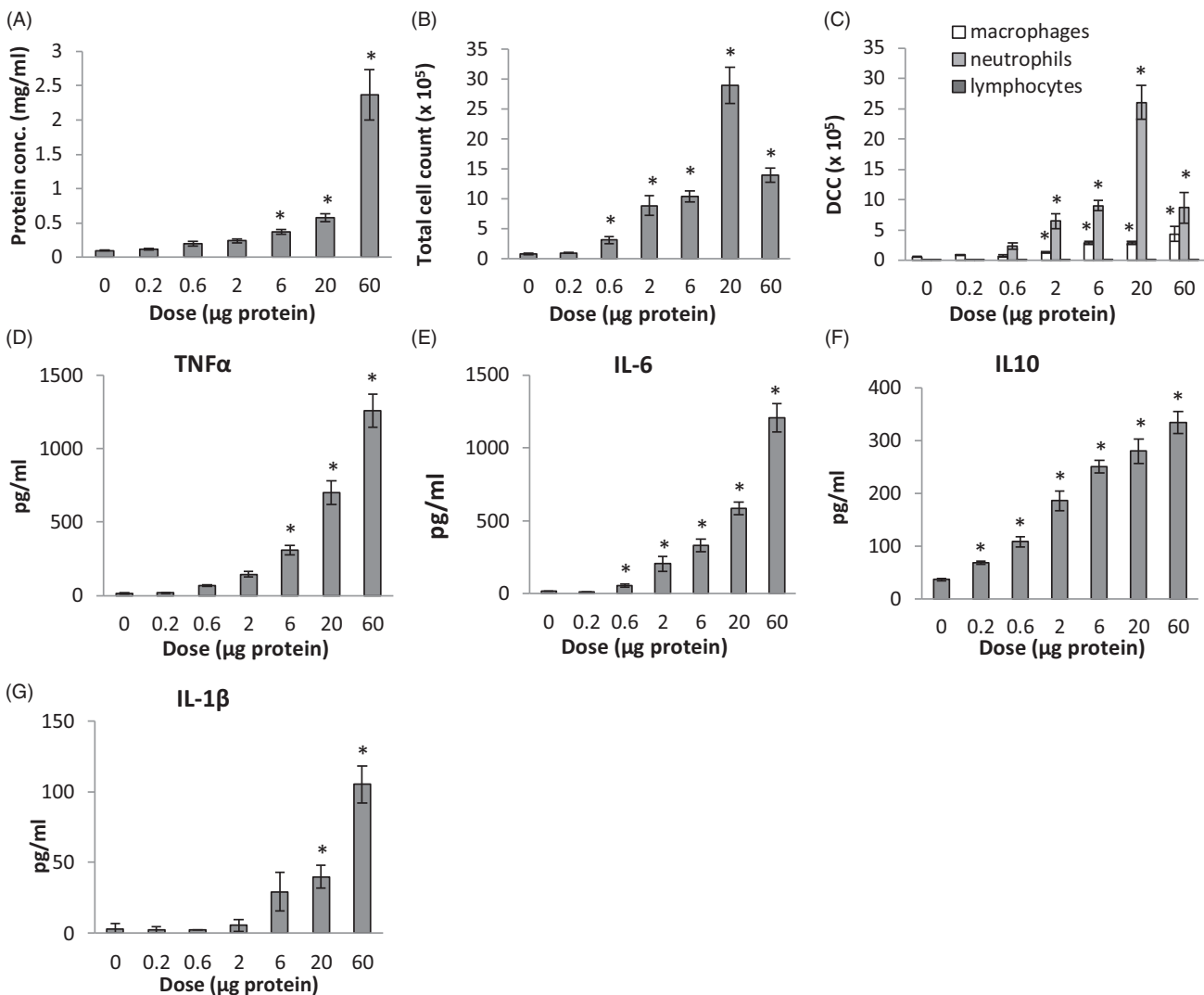


Figure 3. Dose-dependent cytokine response in mouse lung after oropharyngeal exposure to increasing doses (in terms of mycobacterial protein) of whole cell lysate of *M. immunogenum* 700506. BALF was collected 4 h post-instillation of final dose. Panels A–C: Biochemical and cellular changes in BALF: (A) Total protein concentration, (B) Total immune cell counts, and (C) Differential cell counts (DCC) of immune cells. Panels D–G: BALF levels of (D) TNF α , (E) IL-6, (F) IL-10, and (G) IL-1 β . *Significantly different from control (0 µg dose) ($p \leq 0.05$).

700506 resulted in the highest average concentration (153 pg/ml), followed by MJY1 and MJY10 at 140 and 135 pg/ml, respectively.

Pathological responses

In general, the inflammation was more extensive in the alveoli (primarily neutrophilic) than in the perivasculär region (primarily lymphocytic). A very mild-to-mild perivasculär, primarily lymphocytic, infiltration was seen in all groups except MJY2 and MJY23 (Figure 9(A)). All groups had mild-to-moderate primarily neutrophilic alveolar infiltration, with no statistically significant differences between the groups. Very mild-to-mild pyogranulomas were found in all groups except MJY2 and MJY25. Granuloma formation tended to be greater in the MI 700506 and *S. rectivirgula* groups, but the differences were not significant. The overall severity of lung lesions was mild-to-moderate, with no significant differences noted between the groups (Figure 9(B)). The overall extensiveness of the lesions was, however, significantly greater in the MJY10 group compared with the other *M. immunogenum* groups (overall ANOVA $p = 0.023$). Among the *M. chelonae* groups, MJY1 had the

greatest extensiveness of lesions, although the difference was not significant.

Discussion

Development of subacute and chronic HP is dependent on cell-mediated immunity involving activation of phagocytes, antigen-specific T-lymphocytes, and the release of various cytokines by both these cell types in response to an antigen (Lacasse et al. 2012). However, consistent occurrence of these immune response events in the same combination and measure in acute HP is unclear. A recent study of five human acute HP cases and three subacute or chronic HP cases with acute exacerbations demonstrated pronounced neutrophilic infiltration, bronchiolocentric inflammation, and/or bronchiolitis obliterans in all eight cases (Hariri et al. 2012). Limited controlled studies using animal models and appropriate causative antigens for farmers' HP have reported events characteristic of acute HP (Schuyler 1993; Hunninghake & Richerson 1998; Schuyler et al. 2000).

In the current study on short-term/acute exposure to mycobacterial antigens known to cause machinists HP, exposure

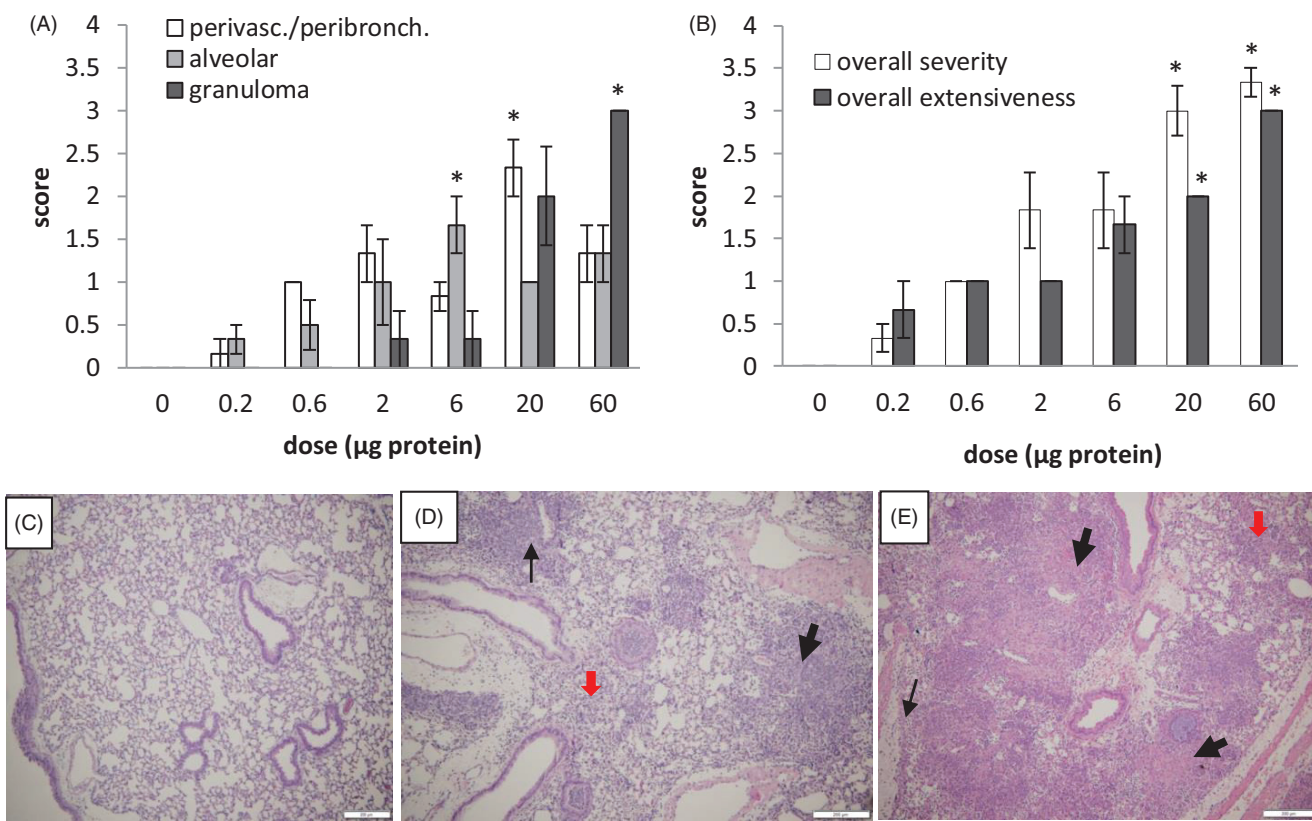


Figure 4. Dose-dependent histopathological changes in the mouse lung after oropharyngeal exposure to increasing doses (μg mycobacterial protein/animal) of whole cell lysate of *M. immunogenum* 700506. Analysis was performed on tissues harvested 4 h post-instillation of final dose. Top panels (A,B): Quantitative changes as measured by overall scores for severity and extensiveness of pathology, as well as scores for specific histopathological changes, assigned on a subjective scale of 0–4 as described in Materials and methods. *Significant difference from control (0 μg dose). Bottom panels (C,D,E): Representative H&E-stained lung sections depicting specific pathological features (shown by arrows) in low dose (6 μg ; panel D) and high dose (60 μg ; panel E)-exposed lungs as compared to in normal lung (vehicle control; panel C). Thick red arrow (alveolar infiltration of histiocytes/neutrophils); thin black arrow (perivascular/peri-bronchiolar infiltration of lymphocytes); thick black arrow (granuloma). Magnification =10 \times .

resulted in robust early IL-6 and TNF α responses but low IFN γ levels (depending on dose type) in the mouse lung. Further, cellularity in BALF and histopathological analyses showed the vast majority of infiltrating cells were neutrophils, with low percentages of lymphocytes, suggesting the cell-mediated adaptive immune system was partially activated. These findings collectively suggest that our short-term exposure mouse model largely mimics the acute HP characteristics.

HP is considered a T_H1-driven disease and Type IV delayed hypersensitivity is a hallmark of subacute and chronic forms of HP. Although still a matter of debate, it has often been suggested that Type III immune complex-driven hypersensitivity responses account for the early stage of acute HP (Kaltreider 1993; McSharry et al. 2002). In support of this, the majority of patients have precipitating antibodies that are specific for the offending antigen (Reboux et al. 2007). This is consistent with our latest report on positive antibody response specific to MI purified recombinant antigens in the serum samples from machinists presenting physician-diagnosed HP (Chandra et al. 2015). While subacute/chronic HP in humans is characterized by strong increases of lymphocytes in BALF and interstitial infiltrate, in acute HP early increases in BALF neutrophils and neutrophilic lung lesions have been noted (Fournier et al. 1985; Hariri et al. 2012), in agreement with a Type III mechanism. Conclusive evidence, however, of a role for immune complexes in HP has not yet emerged.

Release of inflammatory mediators and increases in neutrophils in early phases of microbially-induced acute HP are also

consistent with an innate immune response to pathogen-associated molecular patterns. Since the mice used in this study were immune naïve at the time of instillation, it is likely the innate immune system was largely responsible for the rapid onset of immune responses observed in this model. The early increase of TNF α and IL-6 at 2 h after the final instillation followed by an increase of neutrophils in BALF that peaked between 4 and 12 h was consistent with neutrophils being recruited by TNF α and IL-6, both most likely released by alveolar macrophages (Schuyler et al. 2000). Taken together, the immunopathological observations in the current study using mycobacterial antigen extracts were largely consistent with acute HP pathology in human cases, a pathology characterized by increased neutrophilic infiltrate (Hariri et al. 2012) and an infectious pneumonia-like clinical presentation. However, these comparisons may be somewhat limited by the fact that clinical cases of acute HP may involve pre-sensitization through earlier low-level exposure to the antigen, whereas mice used here were immune naïve.

Role of live intact bacterial cells versus cell lysates in conferring immunogenicity potential

Animal models of HP in general and mycobacterial HP in particular have been based on the use of whole cell extracts (Thorne et al. 2006) or heat-killed cells (Gordon et al. 2006) rather than live microbial cells. It has to be considered, however, that the response to an antigen may depend on the cellular context (intact cell versus lysed cell) in which it is presented to the

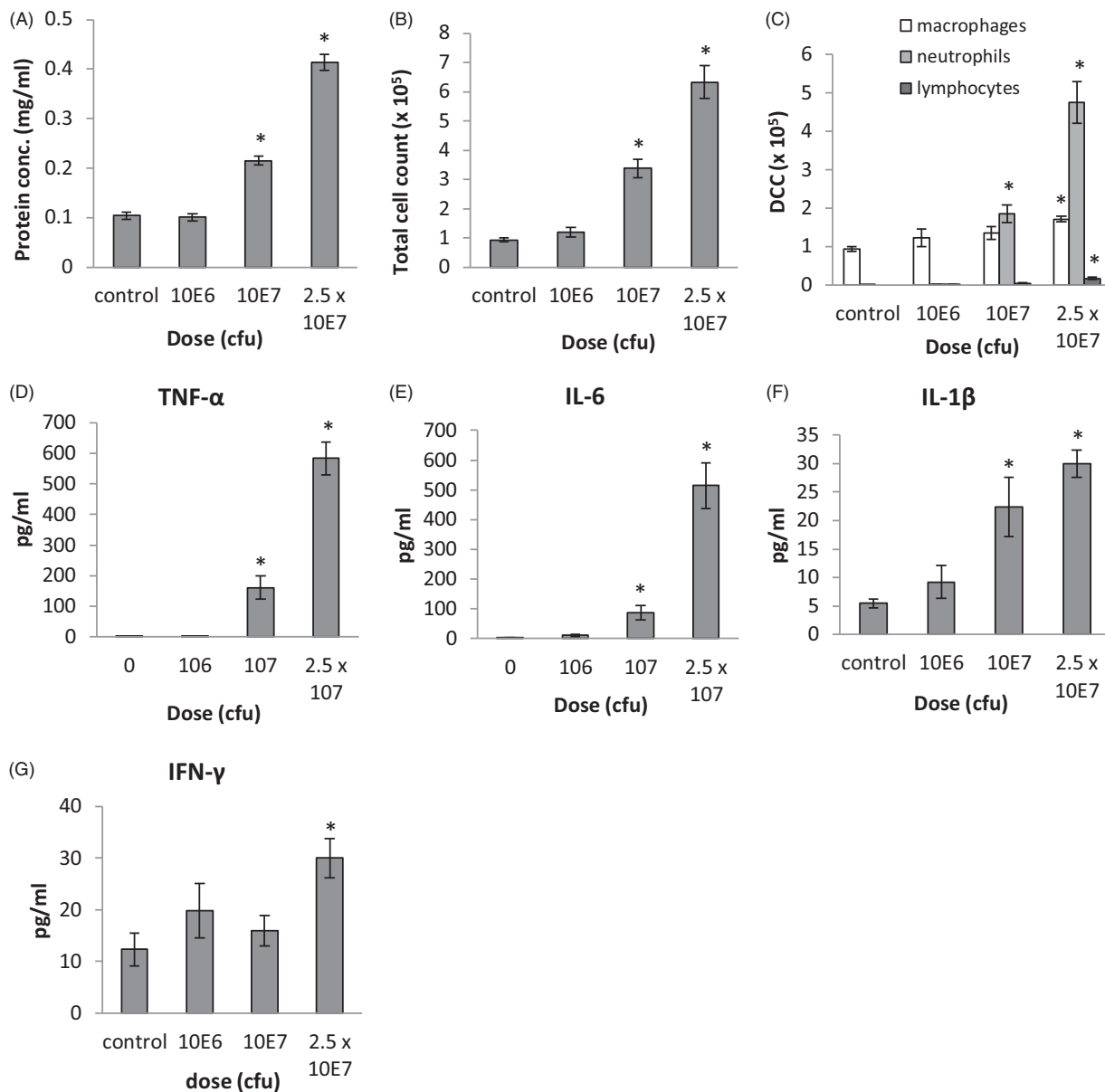


Figure 5. Dose-dependent effect of live cell suspension of *M. immunogenum* 700506 on lung immunological changes. Mice were instilled with increasing doses of monodispersed cell suspension by oropharyngeal inhalation. BALF was collected 4 h post-instillation of final dose. Panels A–C: Biochemical and cellular changes in BALF; (A) Total protein concentration; (B) Total immune cell counts; and, (C) Differential cell counts (DCC) of immune cells. Panels D–G: BALF levels of (D) TNF α , (E) IL-6, (F) IL-10, and (G) IL-1 β . *Significantly different from control (0 cfu dose) ($p \leq 0.05$).

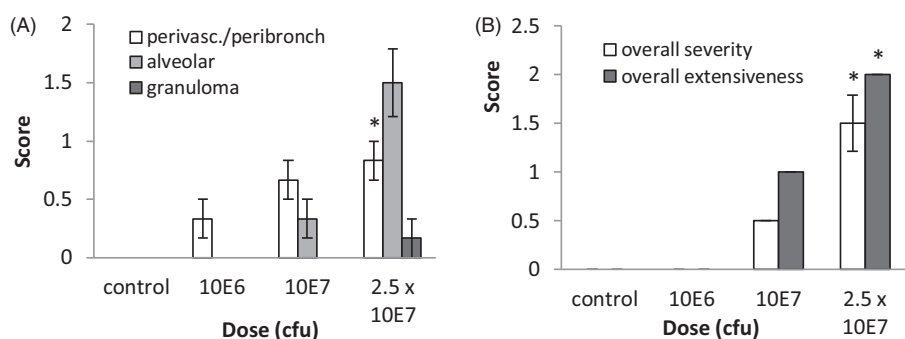


Figure 6. Effect of live cell suspension of *M. immunogenum* 700506 on lung histopathological changes in mice. Increasing dose of monodispersed live cell suspension was administered using oropharyngeal route of exposure. At 4 h post-instillation of final dose, pathological changes in the lung were evaluated in terms of overall scores for severity and extensiveness of damage, as well as scores for specific histopathological changes, assigned on a subjective scale of 0–4 as described in Materials and methods section. *Significantly different from control (0 cfu dose) ($p \leq 0.05$).

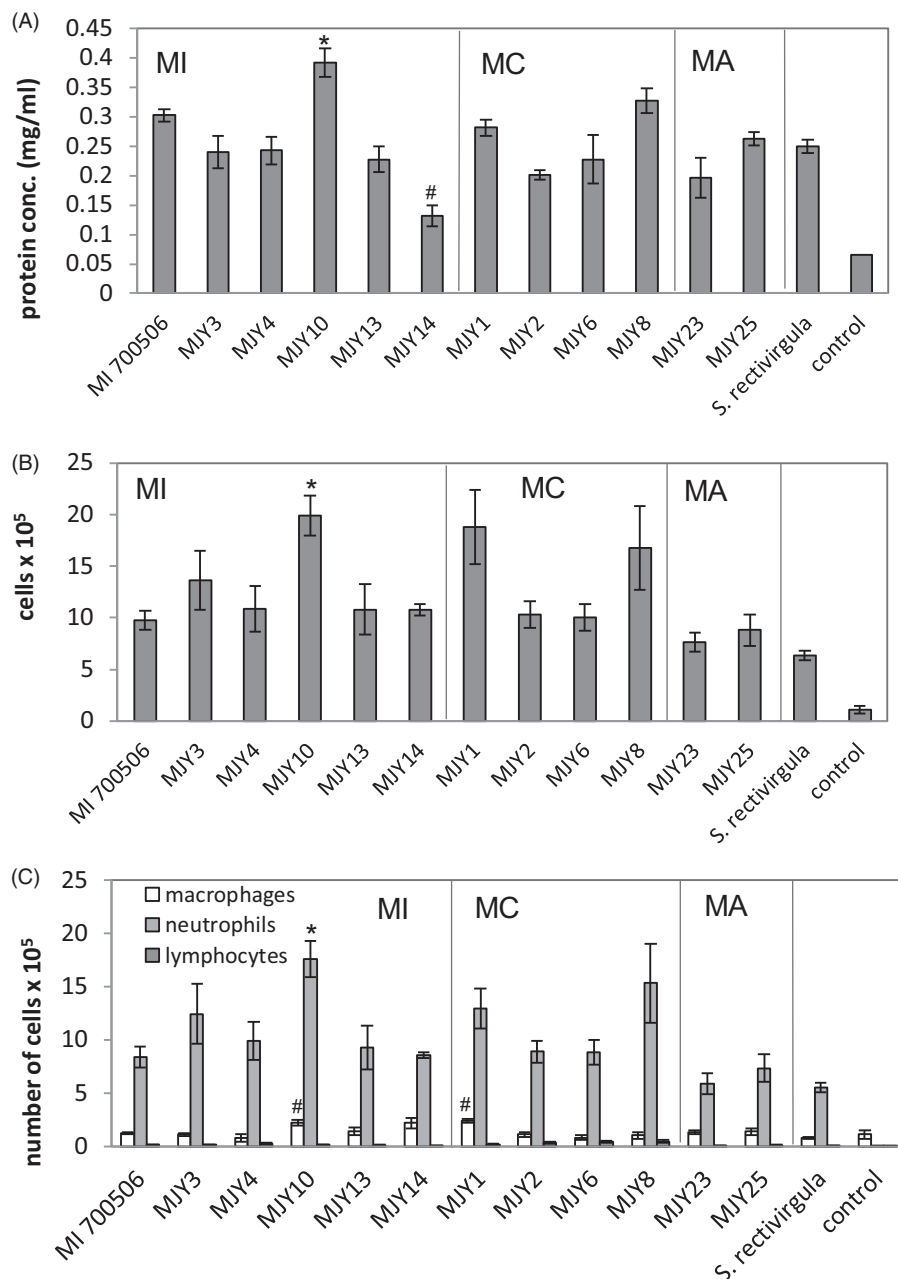


Figure 7. Comparison of individual mycobacterial genotypes/variants (belonging to three different species) for potential to induce cellular changes in BALF of mice after oropharyngeal exposure using whole cell lysates. BALF was collected 4 h post-instillation of final dose and analyzed. (A) Protein concentration: *significantly greater than all other groups except MJY8 and MI 700506, #significantly lower than MI 700506, MJY1, MJY8, MJY10, MJY25, and *S. rectivirgula* groups. (B) Total cell count: *significantly greater than those for groups MI 700506, MJY2, MJY6, MJY13, MJY23, MJY25, and *S. rectivirgula*. (C) Differential cell counts (DCC): *significantly greater neutrophil counts than for MJY2, MJY6, MJY14, MJY23, MJY25, MI 700506, and *S. rectivirgula* groups. The 12 genotypes/variants used belonged to three mycobacterial species, including six *M. immunogenum* genotypes (MI 700506, MJY3, MJY4, MJY10, MJY13, and MJY14), four *M. chelonae* genotypes (MJY1, MJY2, MJY6, and MJY8), and two *M. abscessus* variants/morphotypes (MJY23 and MJY25). Actinomycete *S. rectivirgula* lysate (250 µg/animal) = positive control for comparison. Vehicle (PBS)-treated mice = negative control. *p* < 0.05 considered significant.

immune system (Feng et al. 2010). Furthermore, possible infectivity of viable cells may lead to an altered immune response. In this study, the responses to MI 700506 viable cells and the equivalent amounts of cell extract (lysate) were comparable for majority of the inflammatory cytokine responses except IL-10 (which was not detectably induced by live MI cells). Importantly, only live MI cells induced appreciable levels of IFN γ release and lymphocyte infiltration (as evident from BALF analysis/histopathology). This suggested pre-formed antigens (present in cell extracts) were largely responsible for triggering the acute immune response to short-term airway exposure, whereas viable bacteria may have additionally elicited some cell-mediated adaptive

immune response. This would be consistent with reports documenting that human acute HP (which may involve exposure to both live and dead cells) is primarily marked by neutrophilia, but may also involve some lymphocytosis in the lung (Hunninghake & Richerson 1998; Schuyler et al. 2000).

Differential immunogenic potential of MWF-associated mycobacterial genotypes/variants (inter- and intra-species differences)

While exposure to machining fluids colonized with mycobacteria has been widely linked with incidence of HP in the exposed

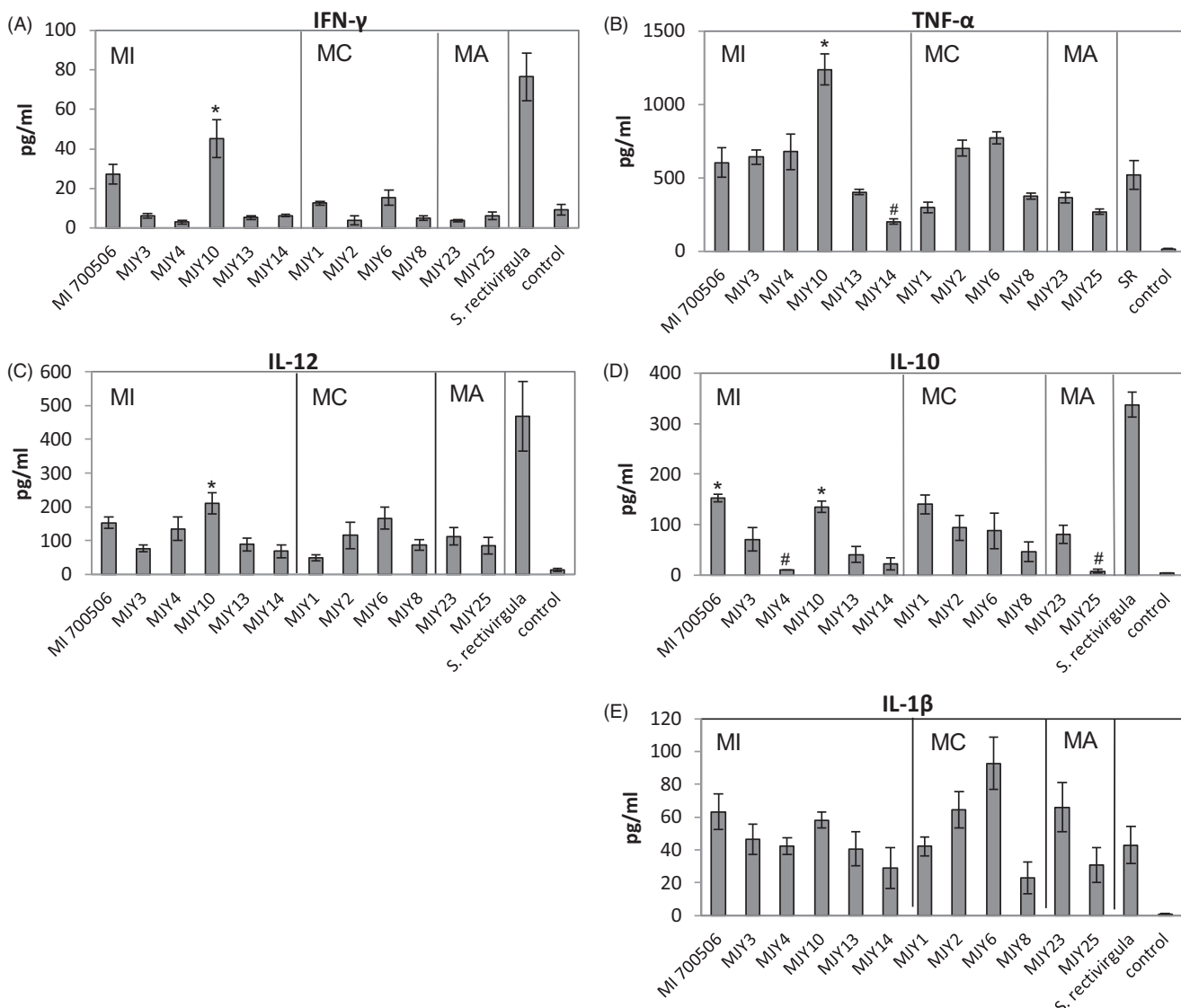


Figure 8. Comparison of individual mycobacterial genotypes/variants (belonging to three different species) for potential to induce cytokine release into BALF of mice after oropharyngeal exposure to whole cell lysates. BALF was collected 4 h post-instillation of final dose and analyzed. (A) IFN γ : *significantly greater than all other groups except MI 700506 and *S. rectivirgula*. (B) TNF α : *significantly greater than for all other groups except MUY2 and MUY6, #significantly lower than all other groups except MUY1, MUY8, MUY23, and MUY25. (C) IL-12: *significantly greater than MUY1 and MUY14 groups. (D) IL-10: *significantly greater than MUY4, MUY8, MUY13, MUY14, MUY25, and *S. rectivirgula*; #significantly lower than MUY1, MUY10, MI 700506, and *S. rectivirgula*. (E) IL-1 β . Test genotypes/variants, comparison control, and vehicle control used were as described in Figure 7. $p < 0.05$ considered significant.

machine workers, there may be no HP cases in machining environments using mycobacteria-containing fluids (Khan et al. 2005; Meza et al. 2013). We hypothesized that differential immunogenicity of MWF-associated mycobacteria strains may be responsible for this disconnect and wanted to test this using the short-term exposure protocol. The mycobacterial genotypes/variants used for the strain comparison in this study all belonged to the cheloneae-abscessus group of rapidly growing non-tuberculous mycobacteria and were previously isolated from used MWF (Khan et al. 2005; Kapoor & Yadav 2012). Since the 16S rRNA gene has limited sequence variability in the cheloneae-abscessus group, a combination of genotyping techniques, including sequencing of a *hsp65* amplicon, phylogenetic analysis of rRNA internal transcribed spaces sequences, and macro-restriction fragment pattern analysis based on pulsed field gel electrophoresis (PFGE), was used to reveal a considerable subspecies diversity among the isolates.

The screening of genotypes/variants showed both inter-species and intra-species differences in immunogenicity potential. In the intra-species comparisons, while the closely related variants

(considered to have the same genotype class based on the PFGE-based genotyping assay employed) showed common response patterns, limited immune response differences between these variants were also observed. For instance, the *M. immunogenum* variants MUY13 and MUY14 used here were identical with regard to the PFGE characterized genotype class; the immune responses to these two variants were not statistically different for various parameters except BALF total protein and TNF α levels. Similarly, *M. cheloneae* variants MUY1 and MUY8 were also identical with regard to characterized genotype; immune responses to these variants were of similar magnitude for all parameters except for extensiveness of lung lesions and IL-10 levels. Such limited immune response differences between closely-related variants (with matching pattern on PFGE-based genotyping) could be because of subtle genomic differences undetectable by the PFGE genotyping approach originally employed for genotype assignment (Khan et al. 2005).

Among the *M. immunogenum* genotypes, MUY10 had the highest immune responses and also the most extensive lung

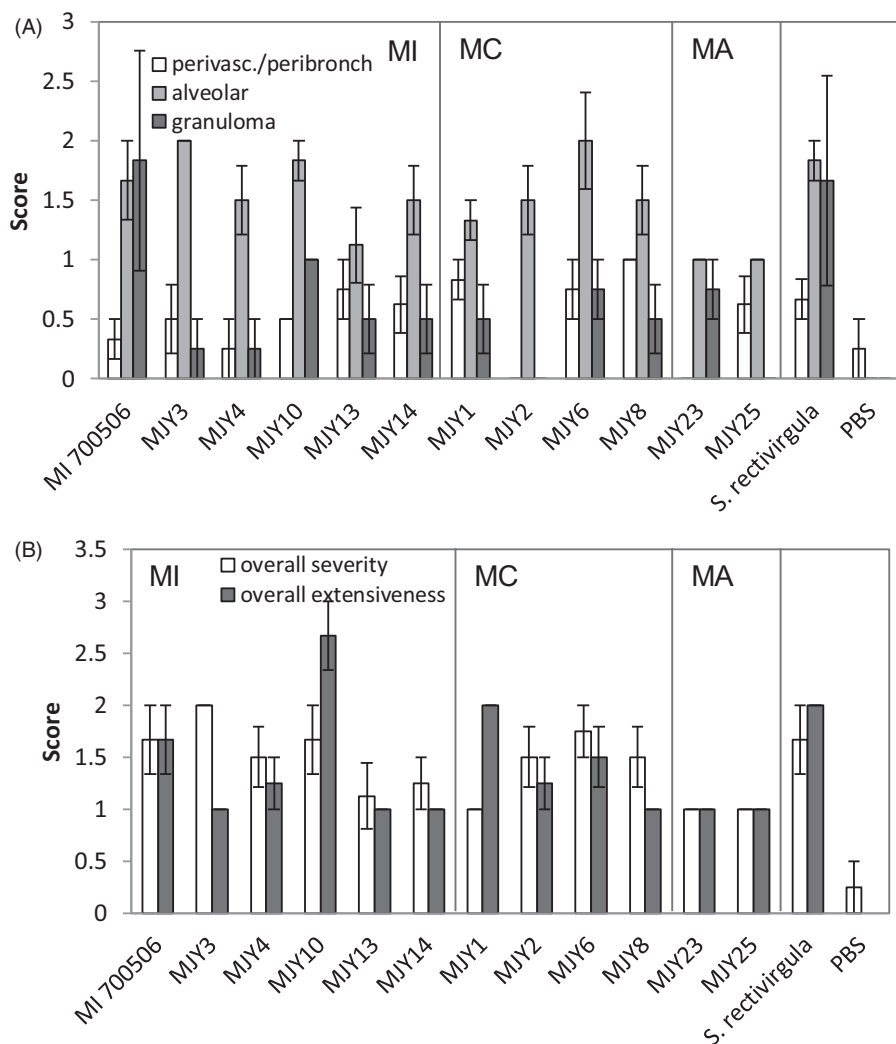


Figure 9. Comparison of individual mycobacterial genotypes/variants (belonging to three different species) for potential to induce histopathological changes in mouse lung after oropharyngeal exposure to whole cell lysates. At 4 h post-instillation of final dose, pathological changes in the lung were evaluated in terms of overall scores for severity and extensiveness of damage (Panel B), as well as scores for specific histopathological changes (Panel A), assigned on a subjective scale of 0–4 as described under Materials and methods section. Test genotypes/variants, comparison control, and vehicle control used were as described in Figure 7.

lesions, and MJY13 and MJY14 tended to be the lowest inducers for several parameters, mainly TNF α levels and extensiveness of lung lesions (MJY3 and MJY4 also tended to match MJY13/14 for induction of cytokines). There was no clear trend for the most immunogenic genotype in *M. chelonae* although MJY1, MJY6 and MJY8 tended to induce higher response for different sets of parameters. MJY23 showed relatively higher immunogenicity potential in many respects as compared with MJY25 within the *M. abscessus* species. This was consistent with a higher virulence of rough morphotype (colony morphology variant) as compared with smooth variant of this species in infection-based models, ascribed to reduced expression of glycopeptidolipids in the cell wall of rough colony variants (Howard et al. 2006). Overall, MJY10 showed the highest immunogenic potential among all the genotypes/variants from the three species.

The results from this study on the characterized genotype/variants (and future studies using chronic HP models) may aid in identifying HP-causative antigenic proteins by comparing the most immunogenic with the least immunogenic genotypes using differential immunological (Mundt et al. 1996) and modern

immunoproteomic (Gupta et al. 2009; Roussel et al. 2011) profiling. Such identified antigens may become useful tools in diagnosis, and may also help the search for therapeutic interventions against HP induced by mycobacteria in MWFs.

Conclusions

The current study characterized a short-term exposure mouse model of mycobacterial HP showing pathology mimicking human cases of acute HP. Specifically, the observed early onset of immune-pathological response that resolved within 4 days in this model mimicked the early events and transient immune response characteristic of human acute HP. The mouse model enabled meaningful profiling of various genotypes/variants of MWF-isolated mycobacteria species for their relative immunogenic potential and thus could serve as a useful tool for routine screening of such isolates for an early risk assessment and timely intervention in the industrial workplace. The exposure model is expected to facilitate development of diagnosis and therapeutic strategies for mycobacterial HP in machinists.

Acknowledgements

This study was supported by grant 2R01OH007364 (to JSY) from the National Institute for Occupational Safety and Health (NIOSH), the Centers for Disease Control and Prevention (CDC). The publication cost was met by the University of Cincinnati College of Medicine Dean's Bridge funding (to JSY).

Disclosure statement

The authors declare no conflicts of interest. The authors alone are responsible for the content of this manuscript.

Funding

National Institute for Occupational Safety and Health [2R01OH007364], the Centers for Disease Control and Prevention.

References

- Beckett W, Kallay M, Sood A, Zuo Z, Milton D. 2005. Hypersensitivity pneumonitis associated with environmental mycobacteria. *Environ Health Perspect.* 113:767–770.
- Burton C, Crook B, Scaife H, Evans G, Barber, C. 2012. Systematic review of respiratory outbreaks associated with exposure to water-based metalworking fluids. *Ann Occup Hyg.* 56:374–388.
- Chandra H, Yadav E, Yadav J. 2013. Alveolar macrophage response to the hypersensitivity pneumonitis pathogen *Mycobacterium immunogenum* is genotype-dependent and is mediated via JNK and p38 MAPK pathways. *PLoS One.* 8:e83172.
- Chandra H, Lockey J, Yadav, J. 2015. Novel antigens of *Mycobacterium immunogenum* relevant for serodiagnosis of hypersensitivity pneumonitis in machinists. *Ann. Allergy Asthma Immunol.* 114:525–526.
- Costabel U, Bonella F, Guzman J. 2012. Chronic hypersensitivity pneumonitis. *Clin. Chest Med.* 33:151–163.
- Denis M, Cormier Y, Fournier M, Tardif J, Laviollette M. 1991. Tumor necrosis factor plays an essential role in determining hypersensitivity pneumonitis in a mouse model. *Am J Respir Cell Mol Biol.* 5:477–483.
- Falkingham J. 2003. Mycobacterial aerosols and respiratory disease. *Emerg Infect Dis.* 9:763–767.
- Feng X, Zhang N, Tuo W. 2010. *Neospora caninum* tachyzoite- and antigen-stimulated cytokine production by bone marrow-derived dendritic cells and spleen cells of naive BALB/c mice. *J Parasitol.* 96:717–723.
- Fournier E, Tonnel A, Gosset P, Wallaert B, Ameisen J, Voisin, C. 1985. Early neutrophil alveolitis after antigen inhalation in hypersensitivity pneumonitis. *Chest.* 88:563–566.
- Freeman A, Lockey J, Hawley P, Biddinger P, Trout D. 1998. Hypersensitivity pneumonitis in a machinist. *Am J Ind. Med.* 34:387–392.
- Gordon T, Nadziejko C, Galdanes K, Lewis D, Donnelly K. 2006. *Mycobacterium immunogenum* causes hypersensitivity pneumonitis-like pathology in mice. *Inhal Toxicol.* 18:449–456.
- Grunes D, Beasley M. 2013. Hypersensitivity pneumonitis: A review and update of histologic findings. *J Clin Pathol.* 66:888–895.
- Gudmundsson G, Hunninghake G. 1998. IFN γ is necessary for expression of hypersensitivity pneumonitis. *J Clin Investig.* 99:2386–2390.
- Gupta M, Subramanian V, Yadav J. 2009. Immunoproteomic identification of secretory and subcellular protein antigens and functional evaluation of the secretome fraction of *Mycobacterium immunogenum*, a newly recognized species of the *Mycobacterium chelonae*-*Mycobacterium abscessus* group. *J Proteome Res.* 8:2319–2330.
- Hariri L, Mino-Kenudson M, Shea B, Digumarthy S, Onozato M, Yagi Y, Fraire A, Matsubara O, Mark E. 2012. Distinct histopathology of acute onset or abrupt exacerbation of hypersensitivity pneumonitis. *Human Pathol.* 43:660–668.
- Howard S, Rhoades E, Recht J, Pang X, Alsup A, Kolter R, Lyons C, Byrd T. 2006. Spontaneous reversion of *Mycobacterium abscessus* from a smooth to a rough morphotype is associated with reduced expression of glycopeptidolipid and re-acquisition of an invasive phenotype. *Microbiology.* 152:1581–1590.
- Hunninghake G, Richerson H. 1998. Hypersensitivity pneumonitis and eosinophilic pneumonias. In: Fauci A, Braunwald E, Isselbacher K, Wilson J, Martin J, Kasper D, Hpuser S, Longo D, editors. *Harrison's principles of internal medicine.* 14th ed. New York: McGraw Hill; p. 1426–1429.
- Jimenez-Alvarez L, Zúñiga J, Gaxiola M, Checa M, Becerril C, Mendoza F, Pardo A, Selman M. 2010. Inflammatory response and dynamics of lung T-cell subsets in T_H1, T_H2 biased and T_H2 deficient mice during development of hypersensitivity pneumonitis. *Exp Mol Pathol.* 88:407–415.
- Kaltreider H. 1993. Hypersensitivity pneumonitis. *West J Med.* 159:570–578.
- Kapoor R, Yadav J. 2012. Expanding the mycobacterial diversity of metalworking fluids (MWF): Evidence showing MWF colonization by *Mycobacterium abscessus*. *FEMS Microbiol Ecol.* 79:392–399.
- Khan I, Selvaraju S, Yadav J. 2005. Occurrence and characterization of multiple novel genotypes of *Mycobacterium immunogenum* and *Mycobacterium chelonae* in metalworking fluids. *FEMS Microbiol Ecol.* 54:329–338.
- Kreiss K, Cox-Ganser J. 1997. Metalworking fluid-associated hypersensitivity pneumonitis: A workshop summary. *Am J Ind Med.* 32:423–432.
- Lacasse Y, Girard M, Cormier Y. 2012. Recent advances in hypersensitivity pneumonitis. *Chest.* 142:208–217.
- McSharry C, Anderson K, Bourke S, Boyd G. 2002. Takes your breath away – the immunology of allergic alveolitis. *Clin Exp Immunol.* 128:3–9.
- Meza F, Chen L, Hudson N. 2013. Investigation of respiratory and dermal symptoms associated with metalworking fluids at an aircraft engine manufacturing facility. *Am J Ind Med.* 56:1394–1401.
- Mohr L. 2004. Hypersensitivity pneumonitis. *Curr Opin Pulm Med.* 10:401–411.
- Moore J, Christensen M, Wilson R, Wallace R, Zhang Y, Nash D, Shelton B. 2000. Mycobacterial contamination of metalworking fluids: Involvement of a possible new taxon of rapidly growing mycobacteria. *Am Ind Hyg Assoc J.* 61:205–213.
- Mundt C, Becker W, Schlaak M. 1996. Farmer's lung: patients' IgG₂ antibodies specifically recognize *Saccharopolyspora rectivirgula* proteins and carbohydrate structures. *J Allergy Clin Immunol.* 98:441–450.
- Nance S, Cross R, Fitzpatrick E. 2004. Chemokine production during hypersensitivity pneumonitis. *Eur J Immunol.* 34:677–685.
- Nance S, Cross R, Yi A, Fitzpatrick E. 2005. IFN γ production by innate immune cells is sufficient for development of hypersensitivity pneumonitis. *Eur J Immunol.* 35:1928–1938.
- Reboux G, Piarroux R, Roussel S, Millon L, Bardonnet K, Dolphin J. 2007. Assessment of four serological techniques in the immunological diagnosis of Farmers' lung disease. *J Med Microbiol.* 56:1317–1321.
- Rosenman K. 2009. Asthma, hypersensitivity pneumonitis and other respiratory diseases caused by metalworking fluids. *Curr Opin Allergy Clin Immunol.* 9:97–102.
- Roussel S, Rognon B, Barrera C, Reboux G, Salamin K, Grenouillet F, Thaon I, Dolphin J, Tillie-Leblond I, Quadroni M, et al. 2011. Immunoreactive proteins from *Mycobacterium immunogenum* useful for serodiagnosis of metalworking fluid hypersensitivity pneumonitis. *Int J Med Microbiol.* 301:150–156.
- Schuyler M. 1993. Lessons from hypersensitivity pneumonitis. *West J Med.* 159:620–622.
- Schuyler M, Gott K, Cherne A. 2000. Mediators of hypersensitivity pneumonitis. *J Lab Clin Med.* 136:29–38.
- Schuyler M, Gott K, Edwards B, Nikula, K. 1994. Experimental hypersensitivity pneumonitis. Effect of CD4 cell depletion. *Am J Respir Crit Care Med.* 149:1286–1294.
- Selman M, Buendia-Roldan I. 2012. Immunopathology, diagnosis, and management of hypersensitivity pneumonitis. *Semin Respir Crit Care Med.* 33:543–554.
- Selman M, Pardo A, King, T. 2012. Hypersensitivity pneumonitis: Insights in diagnosis and pathobiology. *Am J Respir Crit Care Med.* 186:314–324.
- Thorne P, Adamcakova-Dodd A, Kelly K, O'Neill M, Duchaine C. 2006. Metalworking fluid with mycobacteria and endotoxin induces hypersensitivity pneumonitis in mice. *Am J Respir Crit Care Med.* 173:759–768.
- Tillie-Leblond I, Grenouillet F, Reboux G, Roussel S, Chouraki B, Lorthois C, Dolphin J, Wallaert B, Millon L. 2011. Hypersensitivity pneumonitis and metalworking fluids contaminated by mycobacteria. *Eur Respir J.* 37:640–647.
- Wilson R, Steingrube V, Böttger E, Springer B, Brown-Elliott B, Vincent V, Jost K, Zhang Y, Garcia M, Chiu S, et al. 2001. *Mycobacterium immunogenum* sp. nov., a novel species related to *Mycobacterium abscessus* and associated with clinical disease, pseudo-outbreaks and contaminated metalworking fluids: An international cooperative study on mycobacterial taxonomy. *Int J Syst Evol Microbiol.* 51:1751–1764.
- Zacharisen M, Kadambi A, Schlueter D, Kurup V, Shack J, Fox J, Anderson H, Fink J. 1998. The spectrum of respiratory disease associated with exposure to metalworking fluids. *J Occup Environ Med.* 40:640–647.